Electrical detection of DC spin current propagation through an epitaxial antiferromagnetic NiO layer

D. G. Newman[1], M. Dąbrowski[1], P. S. Keatley[1], Q. Li[2], M. Yang[2], S. R. Marmion[3], B. J. Hickey[3], Z.-Q. Qiu[2], and R. J. Hicken[1]
[1]Department of Physics and Astronomy, University of Exeter, Exeter, EX4 4QL, United Kingdom
[2]Department of Physics and Astronomy, University of California at Berkeley, Berkeley, California 94720, USA
[3]School of Physics and Astronomy, University of Leeds, Leeds, LS2 9TJ, United Kingdom

A method for detecting dc spin current propagation through an epitaxial antiferromagnetic NiO layer is presented. Spin current is generated by spin pumping from an adjoining ferromagnetic layer and detected in a non-magnetic metallic layer by means of the inverse spin Hall effect. Comparison is made with a YIG/Pt bilayer where only the Pt layer is electrically conducting, but for which spin Hall magnetoresistance makes an additional contribution to the measured signal. The signal obtained from the multilayered stack containing the antiferromagnetic NiO layer is found to contain additional contributions due to anisotropic magnetoresistance. By exciting the sample with out of plane rf magnetic field, and making measurements with a static field applied at different orientations within the plane of the sample, a signal associated with the dc spin current may be identified.

***Index Terms*—Inverse spin Hall effect, spin currents, antiferromagnets.**

I. Introduction

PURE spin currents have attracted great interest due to their potential for energy efficient transfer of information. A pure spin current may be generated by precessional spin pumping, whereby spin angular momentum diffuses from a ferromagnetic source layer undergoing ferromagnetic resonance (FMR) into an adjacent spacer layer [1]. Spin current transmitted through the spacer layer has both ac and dc components. The ac component has been detected by measuring the spin transfer torque (STT) that it exerts on a ferromagnetic (FM) sink layer in X-ray ferromagnetic resonance (XFMR) experiments [2]. The dc component has been detected through the current generated in a metallic sink layer with a large spin Hall angle by means of the inverse spin Hall effect (ISHE) [3]. In the simplest case, from an electrical point of view, the source layer is an insulating ferrimagnet, and there is no ferromagnetic sink layer, as in the case of YIG/Pt [4, 5]. Recently antiferromagnetic (AFM) spacer layers have received increasing attention following the remarkable observation that the transmitted spin current can be enhanced for NiO layers of specific thickness within a YIG/NiO/Pt structure [6], with different microscopic mechanisms being proposed for the propagation of the spin current [7, 8].

Studies of epitaxial AFM layers can provide additional insight because the magnetic order within the AFM is more clearly defined. Recently XFMR has been used to characterise the propagation of ac spin current through both CoO [9] and NiO [10] spacer layers. The latter study showed that ac spin current is enhanced for NiO thicknesses < 6 nm in agreement with a theory based upon the propagation of evanescent AFM spin wave modes [7]. The detection of dc spin current propagation within the same structures has yet to be confirmed. Epitaxial structures designed for XFMR experiments require specific substrates and have relatively complicated multilayered structure. This hinders integration into microscale planar waveguide structures, while ISHE measurements are expected to contain parasitic signals due to other magnetotransport effects. It is therefore unclear whether both ac and dc spin current propagation can be detected in such structures.

In this paper, we perform ISHE measurements on a multilayer structure that contains an AFM NiO(001) layer and in which ac spin current propagation has been previously detected by XFMR measurements [10]. Here, measurements are made in different experimental geometries in order to isolate the ISHE signal from contributions due to anisotropic magnetoresistance (AMR), and comparison is made with a YIG/Pt sample for which no AMR is expected.

Corresponding author: D.G. Newman (email: dn260@exeter.ac.uk).

II. Experiment

A. Sample Fabrication

A MgO(001)/ $Fe_{75}Co_{25}$(5)/Pd(5)/NiO(4)/Fe(1)/$Ni_{81}Fe_{19}$(25)/ MgO(3) structure, with thicknesses in nm, was fabricated by electron beam evaporation at a base pressure below 1×10^{-10} mbar with all layers being epitaxial until the final NiFe (Permalloy, Py) and MgO layers. The NiO(001) was grown on MgO(001) with MgO[100] || FeCo[110] || NiO[100]. For comparison, an epitaxial GGG/YIG(50)/Pt(4) sample was grown by magnetron sputtering. The YIG film was deposited by RF sputtering at ambient temperature from a base pressure of 6.2×10^{-8} Torr, in a 95%:5% Ar:O_2 mixture at a pressure of 2.5 mTorr at a rate of 0.16 Å/s, before being annealed in air for 2 hours at 850°C and allowed to cool to room temperature. Finally, Pt was deposited by DC sputtering at a rate of 0.20 ± 0.01 Å/s [11]. Both samples had square shape with side of length 8mm and 5mm for the YIG/Pt bilayer and NiO multilayer respectively.

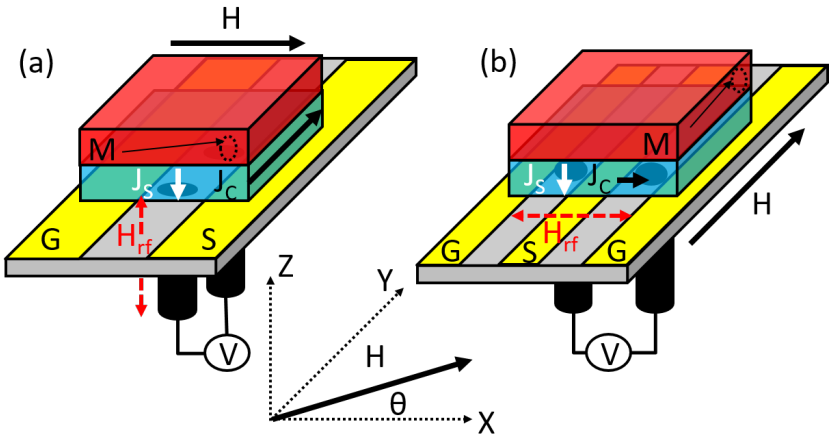

Fig. 1. Experimental geometries used for inverse spin Hall effect (ISHE) measurements with (a) out-of-plane (OoP) and (b) in-plane (IP) rf magnetic field excitation of an overlaid YIG/Pt sample. The signal (S) and ground (G) lines of the planar waveguides and the coordinate system are shown. The precessing magnetisation $\mathbf{M}$ of the YIG (red) layer generates dc spin current $\mathbf{J_S}$ with polarization parallel to the equilibrium magnetization direction, which generates charge current $\mathbf{J_C}$ in the Pt (blue) layer by means of the ISHE. The orientation of the static bias field is $\theta = 0°$ in (a) and $\theta = 90°$ in (b) so that maximum dc voltage V is generated between the black electrical contacts.

B. Inverse spin Hall Effect (ISHE) Measurements

Measurements were performed using two planar waveguide structures, designed to apply either in-plane (IP) or out-of-plane (OoP) rf magnetic field to an overlaid sample, as shown in Fig. 1. The coplanar waveguide (CPW) for IP excitation had ground lines of 2.5mm width and a signal line of 0.5mm width with a 1mm separation, while the coplanar strip (CPS) for OoP excitation had ground and signal lines of 2mm width and 3mm separation. In the former case, the coplanar waveguide had 50 Ohm characteristic impedance and was capable of broadband excitation. In the latter case the coplanar strip structure had characteristic impedance greater than 50 Ohms and exhibited resonances at 4.6 and 6.0 GHz that were used to maximise the strength of the rf magnetic field. An electromagnet mounted on a rotating stage supplied a static magnetic field of magnitude H at different orientations within the plane of the sample. In each case the value of H was swept through the FMR field of the source layer. The precessing source layer magnetization pumps spin current into the adjoining layers, generating charge current in layers such as Pd and Pt, that possess large spin Hall angles, by means of the ISHE [1]. Two pressure contact pins were used to detect the dc voltage V generated, and were oriented as shown in Fig. 1 [12]. The pins used to make electrical contact to the sample were separated by distances of 1.5mm and 3mm for the CPW and CPS respectively. For the CPW, the pins were placed within the two gaps between the signal and ground lines while for the CPS both pins were placed in the single gap between the ground and signal lines. Since the ends of the contact pins were slightly raised above the surface of the planar waveguide, no electrical contact was formed between the sample surface and the ground and signal lines, as was verified by routinely checking the resistance between the ground and signal lines. The amplitude of the rf field was modulated at a frequency of 3141.6 Hz so that the voltage could be detected by means of a lock-in amplifier.

The charge current $\mathbf{J_C}$ generated by a spin current $\mathbf{J_S}$ due to the ISHE is given by [3]

$$\mathbf{J_C} = D_{ISHE}\mathbf{J_S} \times \sigma, \tag{1}$$

where D_{ISHE} is the conversion efficiency and σ is the spin polarisation, which lies antiparallel to the source layer magnetisation $\mathbf{M}$. For the case of OoP excitation in Fig. 1(a) the dc ISHE voltage is expected to have maximum value when $\theta = 0°$ so that $\mathbf{J_C}$ lies along the $\hat{\mathbf{y}}$ axis. For $\theta = \pm 90°$ the dc ISHE voltage is expected to vanish. In contrast, for IP excitation, shown in Fig. 1(b), the ISHE voltage is maximum for $\theta = \pm 90°$ and vanishes for $\theta = 0°$ due to the different orientation of the contact pins.

For samples containing electrically conducting ferromagnetic layers, the measurement of the dc ISHE voltage signal may be complicated by the presence of parasitic signal contributions arising from anisotropic magnetoresistance (AMR) and the anomalous Hall effect (AHE). The rf field can induce eddy currents in the sample that mix with the oscillatory magnetoresistance to produce a rectified dc voltage. Different strategies have been described for isolating the ISHE signal [13–16]. The measured dependence of V upon H exhibits a resonance feature at the FMR condition that can be fitted to the superposition of symmetric and antisymmetric Lorentzian components. The ISHE is expected to contribute only to the symmetric component, but it remains necessary to account for contributions from the AMR and AHE, which depend upon the angle at which the static bias field is applied [14–16]. In fact, only for the case of OoP excitation is it possible to separate the different contributions to the symmetric signal component from their different angular dependence [17, 18].

III. Results and Discussion

A. YIG/Pt bilayer

The dependence of V upon H for the YIG/Pt structure measured in different geometries is shown in Fig. 2. In panel

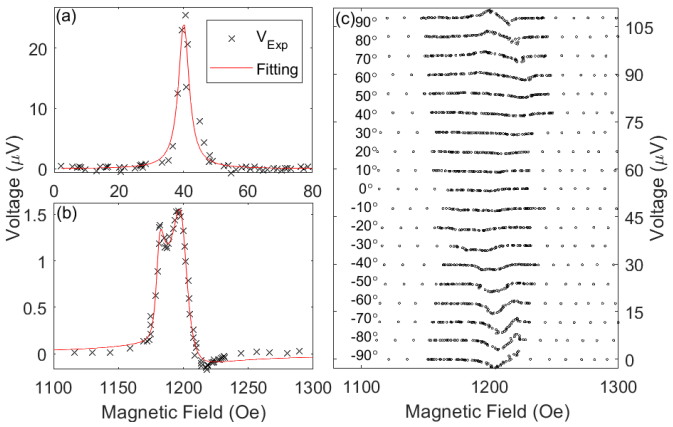

Fig. 2. Measured dc voltage V for the YIG/Pt structure for 22 dBm incident rf power. (a) IP excitation at 1 GHz and static field orientation $\theta = 90°$, fitted to a symmetric Lorentzian function. b) OoP excitation at 4.64 GHz and static field orientation $\theta = 30°$ exhibiting two closely spaced resonances that are each fitted to a superposition of symmetric and antisymmetric Lorentzian functions. c) OoP excitation at 4.64GHz for the static field orientations stated within the figure.

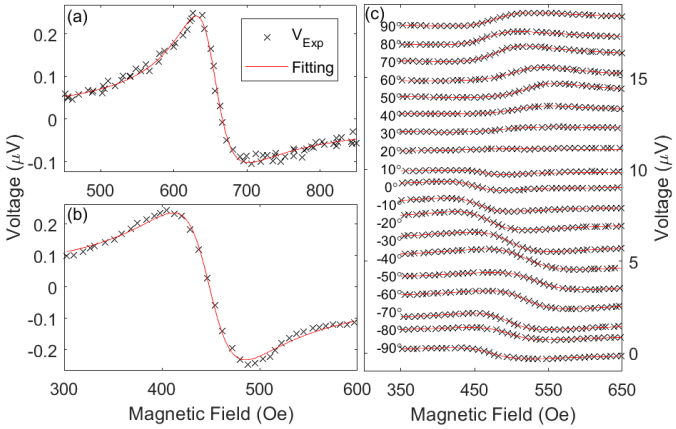

Fig. 3. Measured dc voltage for the structure containing the epitaxial NiO layer for 20 dBm incident rf power. (a) IP excitation at 8 GHz and static field orientation $\theta = 90°$. (b) OoP excitation at 6 GHz and static field orientation $\theta = 0°$. (c) OoP excitation at 6 GHz for the static field orientations stated within the figure. In each panel the experimental data (crosses) is fitted to a superposition of symmetric and antisymmetric Lorentzian functions (red curve).

(a), for IP excitation, the data is well described by a single symmetric Lorentzian function, while the peak height of 30 μV is comparable to values reported previously [5, 16, 19]. Since YIG is an electrical insulator, any AMR or AHE contributions must arise from a proximity effect in the Pt and are therefore expected to be small. However for the epitaxial multilayer to be discussed later, OoP excitation is needed to isolate the ISHE signal, and so further measurements were made upon YIG/Pt with OoP excitation for comparison. In the absence of AMR or AHE, the signal amplitude due to the ISHE is expected to vary as cosθ. Fig. 2 (b) shows a measurement made at an intermediate angle of $\theta = 30°$. Not only does the measured signal contain symmetric and antisymmetric contributions, but the resonance appears to result from the superposition of two closely spaced modes. This splitting of the resonance peak is attributed to spatial inhomogeneity of the sample that becomes more or less apparent depending upon how the sample is positioned upon the waveguide and which complicates the interpretation of the measured signal. Nevertheless, measurements were made with OoP excitation for different field orientations as shown in Fig. 2 (c).

It is immediately apparent that there is an additional much larger asymmetric contribution to the signal that has maximum amplitude at $\theta = \pm 90°$, and which may be tentatively attributed to spin Hall magnetoresistance (SMR) [20]. SMR occurs in YIG/Pt when charge current in the Pt layer generates a spin current, by means of the SHE, that is incident upon the YIG/Pt interface. The amplitude of the back scattered spin current depends upon the orientation of the YIG magnetization, and generates an additional charge current in the Pt that contributes to its apparent electrical resistance [11]. In the present case, the SMR signal results from eddy currents induced in the Pt layer. At the FMR condition, both the amplitude of the current and the spin dependent scattering at the YIG/Pt interface oscillate at the excitation frequency, and mix to produce a dc charge current that contributes to the measured voltage. The spin dependent scattering at the YIG/Pt interface depends upon the relative phase of the spin current and the precession of the YIG magnetization and gives rise to a measured signal of asymmetric shape.

While the mode-splitting of the resonance due to sample inhomogeneity makes detailed analysis of the measured signals impractical, the angular variation of the general size and shape of the signal can be compared with previous reports [20–22]. Other authors have found the SMR contribution to the DC voltage to be an order of magnitude smaller than the ISHE contribution, whereas in the present case the SMR appears to dominate. This may be due to the increased separation (2.5mm) of the ground and signal tracks in the present case and the fact that the sample is overlaid, rather than lithographically defined between the tracks, promoting the excitation of eddy currents. The angular variation of the signal amplitude in Fig. 2(c) suggests a $sin\theta$ dependence, whereas a sinusoidal variation with half the period [20, 22] been reported previously. This suggests that the spatial form of the eddy current distribution is sensitive to geometrical details. In the present case the eddy current density should vanish by symmetry along the middle of the gap between the ground and signal tracks, so presumably some misalignment of the contacts or the sample is required to generate a finite dc voltage by means of SMR.

B. MgO/FeCo/Pd/NiO/Fe/$Ni_{81}Fe_{19}$/MgO multilayer

Within the MgO/FeCo/Pd/NiO/Fe/$Ni_{81}Fe_{19}$/MgO structure, the Fe/Py acts as the source layer and the Pd layer is expected to provide the dominant contribution to the ISHE voltage. The sample was mounted symmetrically across the two electrical contacts to minimise thermal contributions to the measured voltage generated by the FMR or magnetostatic spin waves [14]. All measurements were performed at room temperature, well below the Néel temperature of 5nm NiO film ($T_N >$ 400K).

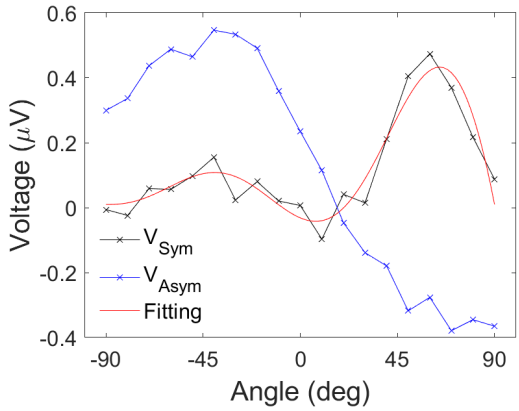

Fig. 4. Amplitudes of the symmetric (black) and antisymmetric (blue) Lorentzians fitted to the data of Fig. 3 (c). The red curve represents a fit of the symmetric data to equation (2).

The dependence of V upon H is shown in Fig. 3 for IP excitation in (a) and for OoP excitation in (b) and (c). In all cases it is necessary to fit the data to the superposition of one symmetric and one antisymmetric Lorentzian function. For the data in Fig. 3 (c), for which the orientation of the static field was varied with OoP rf excitation, the amplitudes of both the symmetric and antisymmetric components are plotted against θ in Fig. 4. As discussed previously, the ISHE should only contribute to the symmetric component of the signal. The amplitude of the symmetric component V_{Sym} has been predicted to vary as [14]

$$V_{Sym} = V_{ISHE}^{OoP} cos(\theta) + V_{AMR}^{OoP(1)} sin(2\theta) + V_{AMR}^{OoP(2)} cos(2\theta) + V_{AMR}^{IP} sin(2\theta) cos(\theta) + V_{AHE}^{OoP}, \quad (2)$$

where the coefficients V_{ISHE}^{OoP}, $V_{AMR}^{OoP(1)}$ and $V_{AMR}^{OoP(2)}$ represent the strength of the contributions from the ISHE and AMR respectively for OoP excitation. It is expected that the OoP induced AMR will manifest two components with angular dependences of $sin(2\theta)$ and $cos(2\theta)$, as in [14], due to the presence of rf current with different spatial components. However other authors have noted [17] that it is also necessary to include an additional term with coefficient V_{AMR}^{IP} that represents an AMR signal generated by an in-plane rf field. This term may be necessary because the electrical contacts are slightly misaligned from the centre of the coplanar structure in Fig. 1 (b), and so experience a small but finite in-plane rf field component. The V_{AHE}^{OoP} coefficient represents the contribution resulting from the AHE. No angular dependence is expected as the static field is rotated within the sample plane rotation with OoP excitation [14].

The values of the voltage coefficients obtained by fitting equation 2 to the symmetric Lorentzian amplitude data in Fig. 3 are shown in table I. The OoP excited ISHE provides the largest contribution to V_{Sym}, although the other terms have significant amplitude. Thermal effects have been shown to introduce signal contributions that can easily be misinterpreted [23, 24]. While they are believed to have negligible effect here, this can only be confirmed by frequency dependent measurements [14] that lie beyond the scope of the present study.

Voltage Coefficent	Angular Form	Fitted value (μV)
V_{ISHE}^{OoP}	cosθ	0.98
$V_{AMR}^{OoP(1)}$	sin2θ	0.49
$V_{AMR}^{OoP(2)}$	cos2θ	-0.51
V_{AMR}^{IP}	sin2θcosθ	-0.57

TABLE I
Fitted values of voltage coefficients for the V_{Sym} data in Fig. 3.

Comparing the size of the signals in Fig. 2 and Fig. 3, it can be seen firstly that the signal is an order of magnitude larger in Fig. 2 (a) compared to Fig. 2 (b). It seems reasonable to assume that the ISHE makes the dominant contribution to the signal in Fig. 2 (b) since the peak shape is largely symmetric, and so panels (a) and (b) indicate the size of the signals due to the ISHE in each case. The signal may be larger in (a) compared to (b) because firstly the rf field is larger for the case of IP excitation due to the use of tracks of smaller width and separation, and secondly, due to the shape anisotropy, rf field with IP orientation induces a more elliptical trajectory with enhanced IP deflection of the magnetization. On the other hand the signals in Fig. 3 (a) and (b) have similar magnitude, but are not easily compared because the ISHE is not necessarily dominant in either case. Comparing Fig.s 2 (b) and 3 (b), the signal amplitude appears to be about a factor of 6 times larger for the YIG/Pt compared to the multilayer containing the NiO layer. Again this is reasonable because firstly the YIG has much smaller linewidth than the Fe/Py and so has larger precession amplitude, secondly Pt is believed to have larger spin Hall angle than Pd, and thirdly, the YIG/Pt does not contain any additional metallic layers that might shunt the current generated by the ISHE.

IV. Conclusion

In summary, we have shown that the dc ISHE voltage generated by spin current propagation through a magnetic multilayer containing epitaxial AFM and metallic FM layers can be detected after care is taken to account for other parasitic signal contributions. Analysis of signals obtained from a seemingly simpler YIG/Pt structure is not necessarily more straightforward due to the presence of sample inhomogeneity and SMR. The presented results pave the way to further studies in which the dependence of dc spin current transmission through epitaxial NiO and CoO layers of different thickness can be explored and compared to XFMR studies of ac spin current transmission.

Acknowledgements

The authors acknowledge the Engineering and Physical Sciences Research Council (EPSRC) under Grant Number EP/P02047X/1. D.G.N acknowledges support via the EPSRC Centre for Doctoral Training in Metamaterials (Grant No. EP/L015331/1).

REFERENCES

[1] Y. Tserkovnyak, A. Brataas, and G. E. W. Bauer, "Enhanced Gilbert Damping in Thin Ferromagnetic Films", Phys. Rev. Lett. **88**, 117601 (2002).

[2] J. Li, L. R. Shelford, P. Shafer, A. Tan, J. X. Deng, P. S. Keatley, C. Hwang, E. Arenholz, G. van der Laan, R. J. Hicken, and Z. Q. Qiu, "Direct detection of pure ac spin current by x-ray pump-probe measurements", Phys. Rev. Lett. **117**, 076602 (2016).

[3] E. Saitoh, M. Ueda, H. Miyajima, and G. Tatara, "Conversion of spin current into charge current at room temperature: inverse spin-hall effect", Applied Physics Letters **88**, 182509 (2006).

[4] C. Hahn, G. de Loubens, M. Viret, O. Klein, V. V. Naletov, and J. Ben Youssef, "Detection of microwave spin pumping using the inverse spin hall effect", Phys. Rev. Lett. **111**, 217204 (2013).

[5] V. Castel, N. Vlietstra, B. J. van Wees, and J. B. Youssef, "Frequency and power dependence of spin-current emission by spin pumping in a thin-film YIG/Pt system", Phys. Rev. B **86**, 134419 (2012).

[6] H. Wang, C. Du, P. C. Hammel, and F. Yang, "Antiferromagnonic spin transport from $Y_3Fe_5O_{12}$ into NiO", Phys. Rev. Lett. **113**, 097202 (2014).

[7] R. Khymyn, I. Lisenkov, V. S. Tiberkevich, A. N. Slavin, and B. A. Ivanov, "Transformation of spin current by antiferromagnetic insulators", Phys. Rev. B **93**, 224421 (2016).

[8] S. M. Rezende, R. L. Rodríguez-Suárez, and A. Azevedo, "Diffusive magnonic spin transport in antiferromagnetic insulators", Phys. Rev. B **93**, 054412 (2016).

[9] Q. Li, M. Yang, C. Klewe, P. Shafer, A. T. N'Diaye, D. Hou, T. Y. Wang, N. Gao, E. Saitoh, C. Hwang, R. J. Hicken, J. Li, E. Arenholz, and Z. Q. Qiu, "Coherent ac spin current transmission across an antiferromagnetic CoO insulator", Nature Communications **10**, 5265 (2019).

[10] M. Dabrowski, T. Nakano, D. M. Burn, A. Frisk, D. G. Newman, C. Klewe, Q. Li, M. Yang, P. Shafer, E. Arenholz, T. Hesjedal, G. van der Laan, Z. Q. Qiu, and R. J. Hicken, "Coherent Transfer of Spin Angular Momentum by Evanescent Spin Waves within Antiferromagnetic NiO", Phys. Rev. Lett. **124**, 217201 (2020).

[11] S. R. Marmion, M. Ali, M. McLaren, D. A. Williams, and B. J. Hickey, "Temperature dependence of spin hall magnetoresistance in thin YIG/Pt films", Phys. Rev. B **89**, 220404 (2014).

[12] D. Wei, M. Obstbaum, M. Ribow, C. H. Back, and G. Woltersdorf, "Spin hall voltages from a.c. and d.c. spin currents", Nature Communications **5**, 3768 (2014).

[13] A. Azevedo, L. H. Vilela-Leão, R. L. Rodríguez-Suárez, A. F. Lacerda Santos, and S. M. Rezende, "Spin pumping and anisotropic magnetoresistance voltages in magnetic bilayers: theory and experiment", Phys. Rev. B **83**, 144402 (2011).

[14] R. Iguchi and E. Saitoh, "Measurement of spin pumping voltage separated from extrinsic microwave effects", Journal of the Physical Society of Japan **86**, 011003 (2017).

[15] M. Harder, Y. Gui, and C.-M. Hu, "Electrical detection of magnetization dynamics via spin rectification effects", Physics Reports **661**, 1 –59 (2016).

[16] H. Zhou, X. Fan, L. Ma, Q. Zhang, L. Cui, S. Zhou, Y. S. Gui, C.-M. Hu, and D. Xue, "Spatial symmetry of spin pumping and inverse spin hall effect in the $Pt/Y_3Fe_5O_{12}$ system", Phys. Rev. B **94**, 134421 (2016).

[17] S. Keller, J. Greser, M. R. Schweizer, A. Conca, V. Lauer, C. Dubs, B. Hillebrands, and E. T. Papaioannou, "Relative weight of the inverse spin-Hall and spin-rectification effects for metallic polycrystalline Py/Pt, epitaxial Fe/Pt, and insulating YIG/Pt bilayers: Angular dependent spin pumping measurements", Phys. Rev. B **96**, 024437 (2017).

[18] M. Obstbaum, M. Härtinger, H. G. Bauer, T. Meier, F. Swientek, C. H. Back, and G. Woltersdorf, "Inverse spin Hall effect in $Ni_{81}Fe_{19}$ normal-metal bilayers", Phys. Rev. B **89**, 060407 (2014).

[19] Z. Qiu, J. Li, D. Hou, E. Arenholz, A. T. N'Diaye, A. Tan, K.-i. Uchida, K. Sato, S. Okamoto, Y. Tserkovnyak, Z. Q. Qiu, and E. Saitoh, "Spin-current probe for phase transition in an insulator", Nature Communications **7**, 12670 (2016).

[20] Q. Zhang, X. Fan, H. Zhou, W. Kong, S. Zhou, Y. S. Gui, C.-M. Hu, and D. Xue, "Investigation of the difference between spin hall magnetoresistance rectification and spin pumping from the viewpoint of magnetization dynamics", Applied Physics Letters **112**, 092406 (2018).

[21] P. Wang, S. W. Jiang, Z. Z. Luan, L. F. Zhou, H. F. Ding, Y. Zhou, X. D. Tao, and D. Wu, "Spin rectification induced by spin hall magnetoresistance at room temperature", Applied Physics Letters **109**, 112406 (2016).

[22] R. Iguchi, K. Sato, D. Hirobe, S. Daimon, and E. Saitoh, "Effect of spin hall magnetoresistance on spin pumping measurements in insulating magnet/metal systems", Applied Physics Express **7**, 013003 (2013).

[23] C. C. Chiang, S. Y. Huang, D. Qu, P. H. Wu, and C. L. Chien, "Absence of Evidence of Electrical Switching of the Antiferromagnetic Néel Vector", Phys. Rev. Lett. **123**, 227203 (2019).

[24] A. Churikova, D. Bono, B. Neltner, A. Wittmann, L. Scipioni, A. Shepard, T. Newhouse-Illige, J. Greer, and G. S. D. Beach, "Non-magnetic origin of spin hall magnetoresistance-like signals in Pt films and epitaxial NiO/Pt bilayers", Applied Physics Letters **116**, 022410 (2020).